

Research Paper

High-throughput functional screening for autophagy-related genes and identification of *TM9SF1* as an autophagosome-inducing gene

Pengfei He,^{1,†} Zhi Peng,^{1,4,†} Ye Luo,¹ Lan Wang,^{2,3} Peng Yu,¹ Weiwei Deng,¹ Yunqing An,⁴ Taiping Shi^{1-3,*} and Dalong Ma¹⁻³

¹Chinese National Human Genome Center; Beijing, China; ²Laboratory of Medical Immunology; School of Basic Medical Science; Peking University Health Science Center; Beijing, China; ³Peking University Center for Human Disease Genomics; Beijing, China; ⁴Department of Immunology; Capital Medical University; Beijing, China

[†]These authors contributed equally to this work.

Abbreviations: TMEM166, transmembrane protein 166; TMEM74, transmembrane protein 74; TM9SF1, transmembrane 9 superfamily member 1; TM9SF3, transmembrane 9 superfamily member 3; GFP, green fluorescent protein; MDC, monodansylcadaverine; LC3, microtubule-associated protein 1 light chain 3; FCS, fetal calf serum; TEM, transmission electron microscopy; PCR, polymerase chain reaction; LTR, lysotracker red; MTR, mitotracker red

Key words: high-throughput screening, autophagy, LC3, TM9SF1, automated fluorescence microscopy system

Autophagy, a tightly regulated process responsible for the bulk degradation of most long-lived proteins and some organelles, is associated with several forms of human diseases including cancer, neurodegenerative disease and cardiomyopathies. However, the molecular machinery involved in autophagy in mammalian cells remains poorly understood. Here, we describe a high-throughput, cell-based functional screening platform, based on an automated fluorescence microscopy system, which enables acquiring and quantitatively analyzing images of GFP-LC3 dots in cotransfected cells. From a library of 1,050 human cDNA clones, we identified three genes (*TM9SF1*, *TMEM166* and *TMEM74*) whose overexpression induced high levels of autophagosome formation. In particular, overexpression of *TM9SF1*, which colocalized with LC3 according to the confocal assay, led to a significant increase in the number of GFP-LC3 dots. The results of transmission electron microscopy and immunoblotting to examine LC3-II levels further confirmed the ability of *TM9SF1* to induce autophagy. Furthermore, knock-down of *TM9SF1* expression by RNA interference could hamper starvation-induced autophagy. The functional screening platform therefore can be applied to high-throughput genomic screening candidate autophagy-related genes, which would provide new insights into underlying molecular mechanisms that may regulate autophagy in mammalian cells.

Introduction

Autophagy, a highly regulated process, is responsible for the bulk degradation of most long-lived proteins and some organelles

and is evolutionarily conserved among eukaryotes.¹⁻³ Autophagy is associated with neurodegenerative disease, cardiomyopathies, cancer, programmed cell death, and bacterial and viral infections.⁴ There are three primary forms of autophagy: macroautophagy, microautophagy and chaperone-mediated autophagy.⁵ Macroautophagy is considered the most prevalent form of autophagy. During macroautophagy (referred to as 'autophagy' hereafter), a cup-shaped structure called the preautophagosome engulfs cytosolic components, including organelles, and closes to form an autophagosome (also known as an 'autophagic vesicle containing undegraded cytoplasm') that subsequently fuses with a lysosome to form an autolysosome, leading to the proteolytic degradation of the internal components of the autolysosome by lysosomal enzymes.⁵

Autophagy has been investigated extensively in yeast, and because of the generation of autophagy-specific mutants in a variety of yeast cell lines, a number of yeast genes involved in autophagy (called 'ATG' genes) have been identified through genetic screens.⁶ In mammalian, although some homologues of yeast ATG genes have been identified and remarkable progress have been made in understanding the molecular mechanisms involved in mammalian autophagy, there are still many questions remained to be answered.^{5,7}

Microtubule-associated protein 1 light chain 3 (LC3), a homologue of yeast Atg8 (Aut7/Apg8), is considered a highly specific marker of autophagosomes.^{8,9} Expression of a green fluorescent protein (GFP) fusion with LC3 (GFP-LC3) and endogenous LC3-II/LC3-I has been used extensively as a specific and sensitive autophagosomal marker used to monitor autophagic activity.⁷ Until now, the GFP-LC3 autophagic marker has never been used in high-throughput assays to identify genes that regulate autophagy due to technical issues associated with the quantification of GFP-LC3 structures in large numbers of samples. Here we demonstrate that the GFP-LC3 structures can be identified and quantified using an automated approach for microscopic data acquisition and analysis using a high-throughput approach.

*Correspondence to: Taiping Shi; Chinese National Human Genome Center; Beijing Functional Genomics Lab 3; #3-707 North YongChang Road BDA; Beijing 100176 China; Tel.: 86.10.67883332; Fax: 86.10.67873016; Email: taiping_shi@yahoo.com.cn

Submitted: 02/19/08; Revised: 10/05/08; Accepted: 10/23/08

Previously published online as an *Autophagy* E-publication:
<http://www.landesbioscience.com/journals/autophagy/article/7247>

In an effort to identify human genes involved in the induction of autophagy, we constructed a high-throughput, cell-based functional screening platform based on an automated fluorescence microscopy system, that enables acquiring and quantitatively analyzing images of GFP-LC3 dots in cotransfected cells. From a library of 1,050 human cDNA clones, we identified three genes (*TM9SF1*, *TMEM166* and *TMEM74*) whose overexpression led to increased numbers of GFP-LC3 dots in the initial screen, which were validated by transmission electron microscopy (TEM) analysis of autophagosome formation and by immunoblot analysis of LC3-II upregulation. Collectively, our data suggest that the genes are likely to play a significant role in autophagy induction. The screening platform we developed for the identification of autophagy-related genes based on automated fluorescence imaging can be applied readily for high-throughput genomic screening using a 384-well plate format or a cellular array, which would facilitate the identification of novel mammalian autophagy-associated genes and the elucidation of underlying molecular mechanisms involved in autophagy induction.

Results

Identification of three candidate genes that induce increased numbers of GFP-LC3 dots. To identify human genes involved in autophagy, we screened 1,050 genes of unknown function from our cDNA library using GFP-LC3 as a marker for autophagosomes (Fig. 1A, Suppl. Table 1). We evaluated the ability of candidate genes to induce autophagy according to the number of GFP-LC3 dots per cell. Cells cotransfected with the empty library vector and the GFP-LC3 vector with and without starvation induction served as positive and negative controls, respectively. The number of GFP-LC3 dots per cell was 0.53 ± 0.14 in negative control (unstarved) cells. For most cDNAs screened, the average number of GFP-LC3 dots per cell was very low (≤ 1.0 for 87.0% of the cDNAs screened). However, the average number of GFP-LC3 dots per cell increased to 2.65 ± 0.43 after starvation induction. Overexpression of three genes (*TM9SF1*, *TMEM166* and *TMEM74*) led to an increased number of GFP-LC3 dots (up to 2.0 per cell; Fig. 1C and D). The function of the three identified genes (*TM9SF1*, *TMEM166* and *TMEM74*) was further confirmed by carrying out three independent experiments (data not shown).

***TM9SF1*-overexpressed HeLa cells contain higher numbers of autophagic and acidic vesicles.** Transmission electron microscopic analysis, which is the primary and universally accepted method for the detection of autophagy,⁷ showed that *TM9SF1*-overexpressed and starving HeLa cells contained extensive numbers of typical autophagic vesicles relative to control cells (Fig. 2A). Therefore, the results of our TEM studies provided additional evidence confirming the ability of *TM9SF1* to induce autophagosome production.

Furthermore, *TM9SF1* overexpression led to increased levels of MDC staining, which is a marker of acid vesicles, in HeLa cells (Fig. 2B). MDC was previously considered a marker for autophagic vacuoles, since it was shown to accumulate in acidic compartments enriched in lipids.¹⁵ However, MDC is no longer considered a specific marker for autophagic vacuoles, because MDC stains acidic cell compartments.^{16,17} The increased levels of MDC staining indicate that *TM9SF1* overexpression induces the formation of acidic vesicles in HeLa cells, which may correspond to acidic autophagic vacuoles or lysosomes.

***TM9SF1* overexpression leads to increased LC3-II levels in HeLa cells.** We found that *TM9SF1*-transfected HeLa cells showed both an increase in the amount of LC3-II and an increase in the LC3-II/LC3-I ratio as determined by immunoblot analysis (Fig. 2C). Furthermore, *TM9SF1* overexpression also led to both an increase in the amount of GFP-LC3-II and an increase in the GFP-LC3-II/GFP-LC3-I ratio (Fig. 2C); this was consistent with our previous results demonstrating that *TM9SF1* overexpression led to an increased number of GFP-LC3 dots and confirmed that *TM9SF1* overexpression induces autophagosome formation.

Previous studies showed that mutation of glycine at position 120 prevents the C-terminal cleavage and the conjugation of LC3 to the autophagosomal membranes.⁹ We found that *TM9SF1* overexpression has no direct effect on aggregate of GFP-LC3(G120A), and GFP-LC3(G120A) was evenly distributed throughout the cell (Fig. 3A). This identified that *TM9SF1* overexpression induces conversion of GFP-LC3-I into GFP-LC3-II but not the aggregation of GFP-LC3 and the puncta are autophagosome-dependent. We also found that lysosomal inhibitor Bafilomycin A1 could significantly increase the dots of GFP-LC3 in *TM9SF1* overexpressed HeLa cells compared with vector overexpressed HeLa cells treated with Bafilomycin A1 (Fig. 3B). The progression of the autophagy is sensitive to the PI3K inhibitors such as wortmannin. We further found that wortmannin could partially inhibit the increment of GFP-LC3 dots caused by *TM9SF1* (Fig. 3C). These results collectively show that *TM9SF1* expression triggers autophagy in HeLa cells.

***TM9SF1* localizes to autophagic vacuoles and lysosome in HeLa cells.** The subcellular localization of proteins is critical to their biological function. Therefore, we determined the subcellular localization of *TM9SF1* using confocal microscopy (Fig. 4). We found that *TM9SF1*-GFP colocalized completely with a DsRed fusion of LC3 (DsRed-LC3), which is associated specifically with autophagic vacuoles. With the treatment of Bafilomycin A1, an inhibitor of the vacuolar proton ATPase, *TM9SF1* still partially colocalized with DsRed-LC3, indicating that *TM9SF1* partially localized to the autophagosome. Furthermore, *TM9SF1*-GFP also colocalized extensively with LTR, which is a sensitive lysosomal/autolysosomal marker. In addition, *TM9SF1* also can colocalize with lysosomal marker LAMP-1. *TM9SF1*-GFP did not colocalize with the mitochondrial marker MTR. In a proteomic analysis of lysosomal integral membrane proteins by Bagshaw et al.¹⁸ *TM9SF1* was found to localize in lysosome, which was consistent with our results. Taken together with the results of our earlier studies, the localization of *TM9SF1* to autophagic vacuoles and lysosome supports a role for *TM9SF1* in autophagy induction.

Knockdown of *TM9SF1* endogenous expression reduces levels of starvation-induced autophagy. To further determine the role of *TM9SF1* in autophagy under physiological conditions, siRNA was designed to knockdown the expression of *TM9SF1* in HeLa cells. Nonsilencing siRNA or siRNA against *TM9SF1* (si-*TM9SF1*) was transfected into HeLa cells alone or combined with the *TM9SF1*-GFP vector. At 48 h after transfection, *TM9SF1* mRNA and protein levels were significantly decreased in cells transfected with si-*TM9SF1*, as assessed by flow cytometry (Fig. 5A), RT-PCR and western blotting (Fig. 5B). To investigate whether si-*TM9SF1* transfected HeLa cells have impact on general lysosomal function,

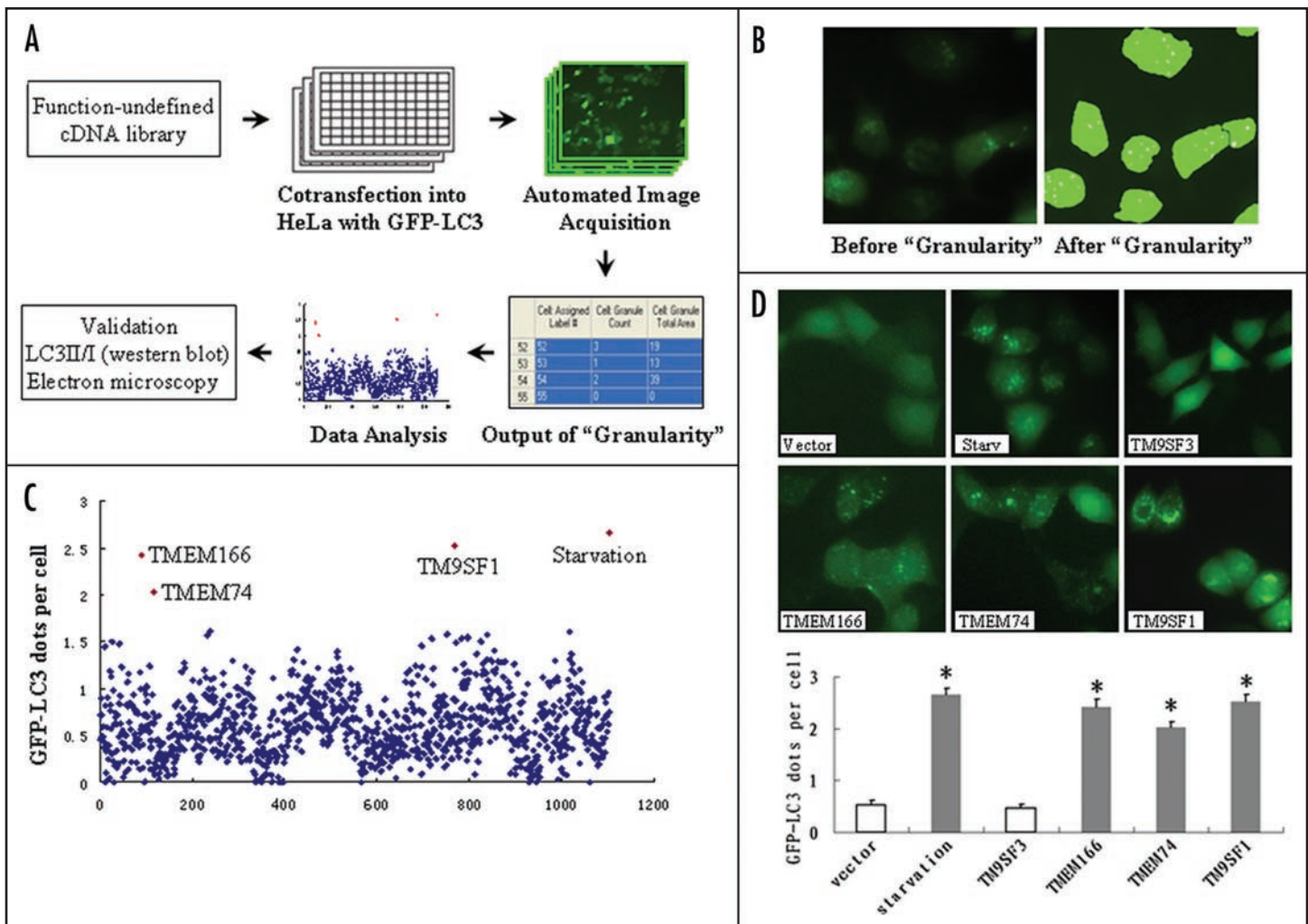


Figure 1. Screening for autophagy-related genes in HeLa cells using GFP-LC3. (A) Work flow of functional screening for autophagy-related genes based on automated fluorescence imaging. (B) "Granularity" module of the MetaMorph 7.0 Imaging System (Molecular Devices, USA). The "granularity" application module is designed to detect and count granules in cells and to measure the physical characteristics of granules. (C) Quantitative analysis of GFP-LC3 dots in HeLa cells overexpressing the gene of unknown function from our cDNA library. The number of GFP-LC3 dots per cell in GFP-LC3-positive cells was determined using the "granularity" application module of the MetaMorph 7.0 Imaging System (Molecular Devices, USA) at 24 h post-transfection. The number of GFP-LC3 dots was counted in at least two independent visual fields from two independent wells. The results were expressed as the average number of GFP-LC3 dots per cell. Starvation (autophagy induced by replacing DMEM medium to Earle's balanced salts solution (EBSS) for HeLa for 12 h) and three "hits" from the cDNA library (*TMEM166*, *TMEM74* and *TM9SF1*) were marked with a red spot. (D) The punctate distribution of GFP-LC3 induced by *TMEM166*, *TMEM74* or *TM9SF1* overexpressed in HeLa cells for 24 h. Negative controls corresponding to the vector alone or to cells expressing an irrelevant membrane protein control (*TM9SF3*: transmembrane 9 superfamily member 3, a homology of *TM9SF1*) did not induce a punctate distribution of GFP-LC3 in HeLa cells. HeLa cells that were cotransfected pcDNA.3.1/myc-His(-)B and GFP-LC3 grown in EBSS for 12 h were set as positive control. Pictures were taken using a 20 \times objective lens. The number of dots per cell of different genes was quantified. Results are the mean \pm SD of three independent experiments. * Significantly different than control, $p < 0.05$.

we detected two major lysosomal proteinases. The result showed no difference in the cathepsin D and acid phosphatase enzymatic activity between nonsilencing and si-TM9SF1 transfected HeLa cells (Fig. 5C). Further, we evaluated whether si-TM9SF1 treatment could inhibit starvation-induced autophagy. HeLa cells transfected with nonsilencing siRNA or si-TM9SF1 were induced by starvation for 2 h to promote autophagy. As illustrated in Figure 5D and E, si-TM9SF1 could inhibit both overexpressed GFP-LC3-II and endogenous LC3-II levels in starved HeLa cells. Furthermore, rescue assay showed knockdown-resistant gene can suppress the defect of the si-TM9SF1 and induce autophagy. While treated with Bafilomycin A1, the LC3-II/LC3-I ratio of non-silencing siRNA

transfected HeLa cells was also significantly increased compared with si-TM9SF1 transfected cells. These data suggest that *TM9SF1* plays a key role in the regulation of cell autophagy.

Discussion

Cellular based large-scale screens have played important roles in elucidating the functions of human genes in a variety of cell signal pathways and in diverse cellular processes.¹⁹⁻²¹ Autophagy is associated with many forms of human diseases.⁴ However, many of the mammalian genes involved in autophagy remain unidentified and studies to monitor autophagy in mammalian cells have only been performed on a small scale.^{7-9,22,23} Therefore, it is necessary

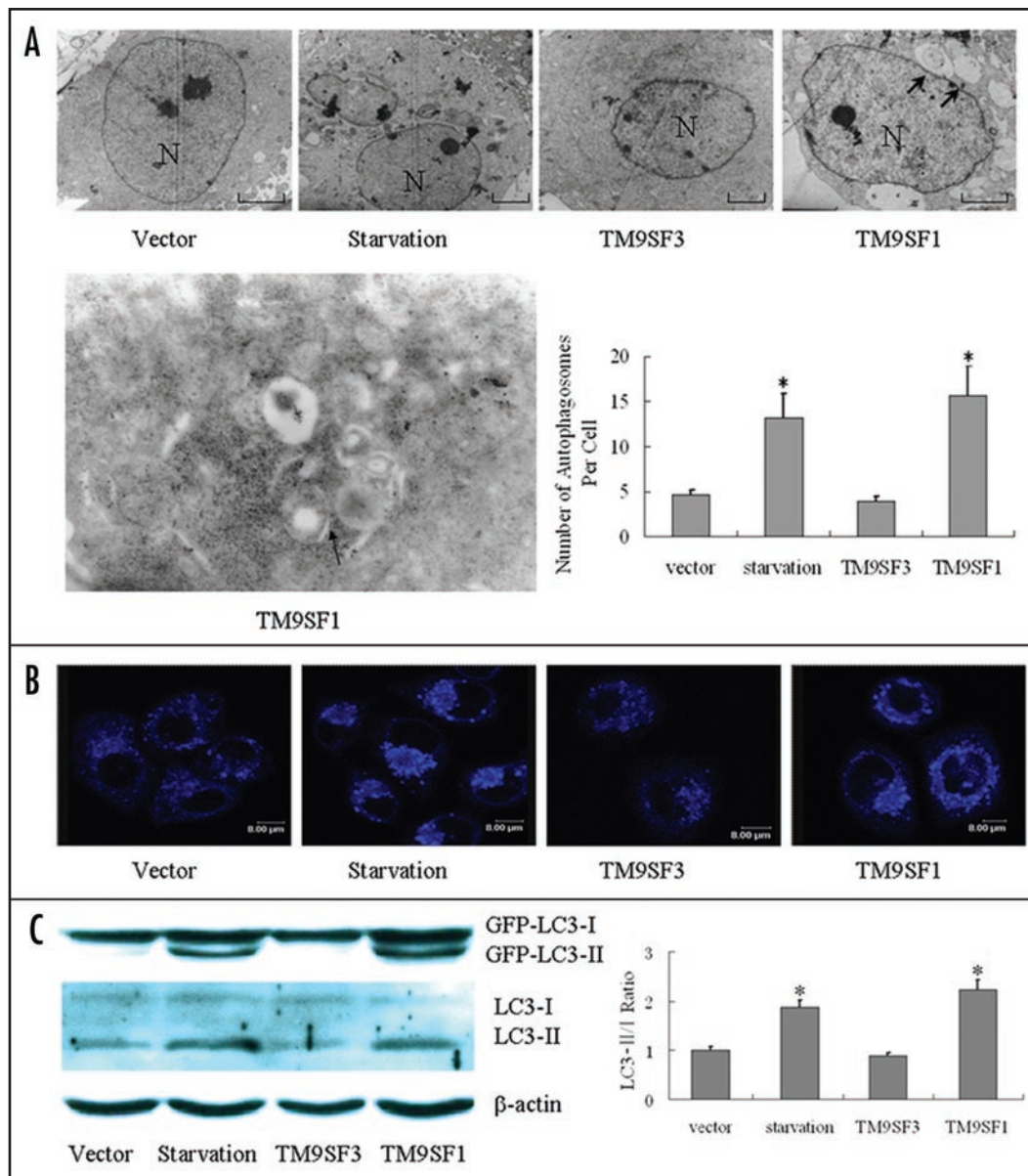


Figure 2. Autophagosomes are accumulated in cells overexpressed *TM9SF1*. (A) Electron microscopic images obtained from transfected HeLa cells. Extensive cytoplasmic vacuolization was observed in starved (starvation) and *TM9SF1*-transfected HeLa cells. A higher magnification (x16,000) image of *TM9SF1* transfected cell was also shown. The number of autophagosomes per cell was quantified by electron microscopy. N, nucleus; arrows indicate autophagosome vacuoles. Scale bars, 2 μ M. (B) *TM9SF1* overexpression led to increased MDC staining in HeLa cells. MDC is used as a marker for acidic cellular vacuoles. The pictures were taken using a 20x microscope objective lens. (C) Increased ratio of GFP-LC3-II/GFP-LC3-I and endogenous LC3-II/LC3-I induced by *TM9SF1* overexpression but not *TM9SF3*. The ratio of cellular LC3-II/LC3-I are shown as the mean \pm SD of three independent experiments. * Significantly different than control, $p < 0.05$.

to establish a platform suitable for large-scale functional screening mammalian genes involved in autophagy.

There are varieties of autophagy detection methods being used in higher eukaryotes, such as quantitative electron microscopy, LC3 and TOR and p62 western blotting, GFP-LC3 and tandem RFP-GFP fluorescence microscopy, and turnover of long-lived proteins, etc.^{24,25} However, many of them are time-consuming and labored. LC3 was identified as a specific and convenient autophagic marker in mammalian cells, and GFP-LC3 was recommended for use in high-throughput functional screens to target autophagy.^{8,9} Examination of GFP-LC3 localization is relatively simple, and requires only a high-resolution fluorescence microscope. In order

to use GFP-LC3 in a high-throughput fluorescence microscopy-based screen, a platform must be established for automated image capture and analysis. Automated fluorescence microscopy imaging and analysis technologies have developed rapidly and have been widely applied in several high-throughput cell image-based screens in recent years.^{19,26} A number of commercial instruments and software are available from well-known companies including Cellomics, Molecular Devices, Axon, Q3DM and GE Health Care.²⁷ Here, we developed an assay to measure autophagy using automated fluorescence microscopy imaging with 96-well plates and an automated fluorescent microscope (Axiovert 200M, Zeiss, Germany) controlled by "scan multiwell plate" and "auto focus" commands

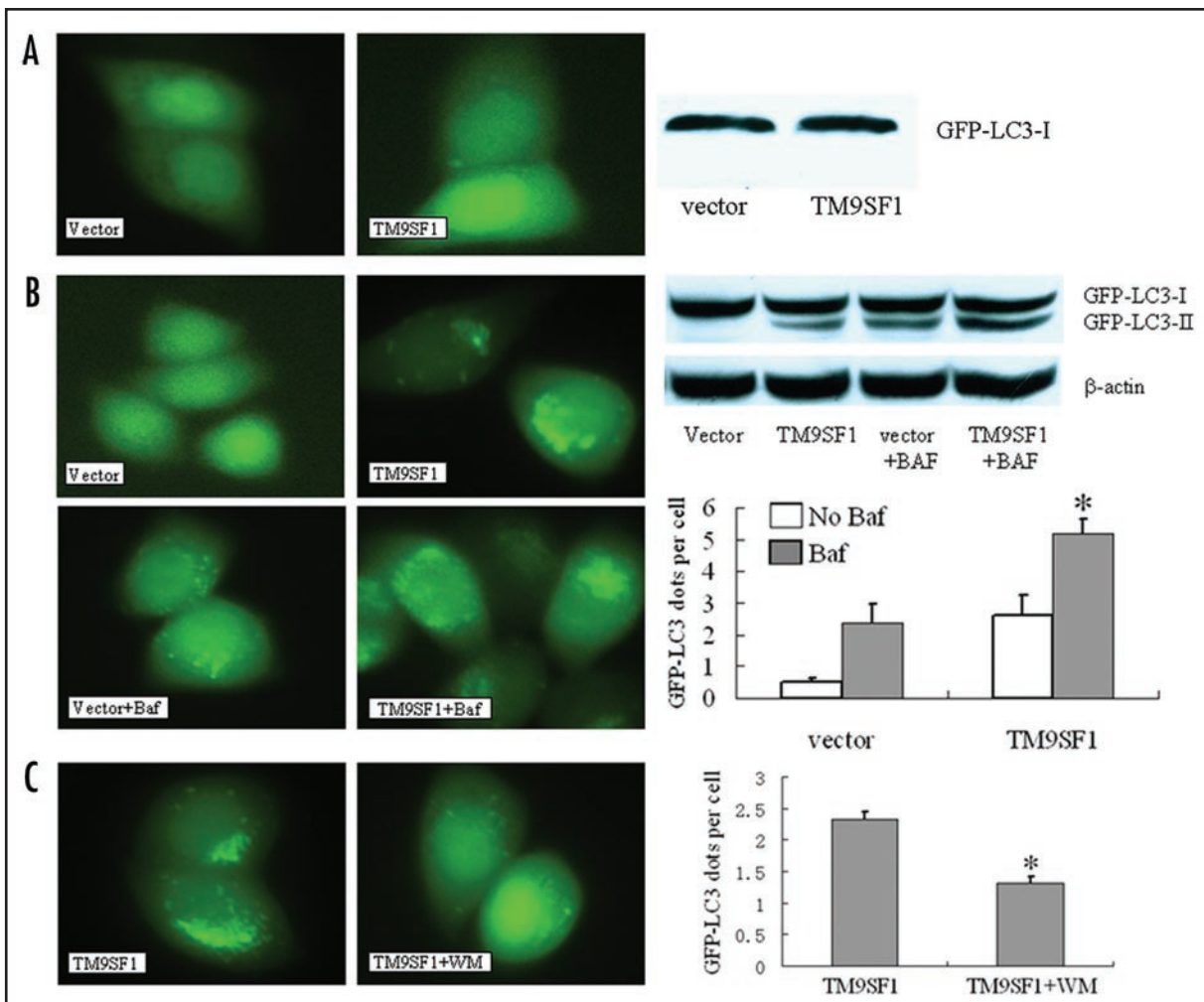


Figure 3. Validation for the autophagy-inducing role of *TM9SF1* by GFP-LC3(G120A), Bafilomycin A1 and wortmannin. (A) overexpression of *TM9SF1* could not induce the aggregate of GFP-LC3(G120A). HeLa cells were transfected GFP-LC3(G120A) and *TM9SF1* (or empty vector). 24 h after transfection, cells were examined under fluorescent microscope (left) or by western blotting using anti-LC3 antibodies (right). (B) After 48 h of transfection, Bafilomycin A1 (100 nM) was added or not added to the cell culture medium. The cells were examined under fluorescent microscope (left). The average number of GFP-LC3 dots per cell was quantified as the mean \pm SD of at least three independent experiments (right). Western blot analysis was also given, which consistent with the GFP-LC3 punctate cells analysis. * Significantly different than control, $p < 0.05$. (C) Increment of GFP-LC3 punctate cells that induced by overexpression of *TM9SF1* could be inhibited by autophagy inhibitor wortmannin. HeLa cells treated with 100 nM wortmannin during co-transfection with GFP-LC3 and *TM9SF1* (or empty vector). After 24 h, the average number of GFP-LC3 dots per cell (left) was determined and expressed as the mean \pm SD of three independent experiments (right). * Significantly different than control, $p < 0.05$.

in the MetaMorph 7.0 Imaging System (Molecular Devices, USA). In addition, we performed an automated image analysis to detect the number of “granules per cell” using the “granularity” application module of MetaMorph 7.0, which is designed to detect and count granules in cells and to measure the physical characteristics of granules. In this study, we developed an effective and convenient screening platform for identifying autophagy-related genes using an automated fluorescence imaging and analysis system, and we screened a library of 1,050 human genes of unknown function and identified three autophagy-related genes. This platform can be applied readily for high-throughput genomic screening using 384-well plates or cellular arrays.

GFP-LC3 was used as an autophagic marker in our screen for autophagy-inducing genes. However, it should be noted that most LC3-positive dots represent preautophagosomes and autophagosomes, rather than autolysosomes.²⁸ The appearance of GFP-LC3

dots or of increasing levels of LC3-II, strictly speaking, does not necessarily correspond to autophagic degradation. Therefore, the autophagy-related genes we identified based on the number of GFP-LC3 dots are considered autophagosome-inducing genes, but not necessarily autophagy-induced genes. Further experimentation, including assays to determine LC3-II turnover suggested by Ise Tanida, will be required to validate the exact roles of the “hits” with respect to autophagy.²⁸

The three initial “hits” from our GFP-LC3-based screen, including *TM9SF1*, *TMEM166* and *TMEM74*, were validated using independent methods to detect autophagy, including TEM, LC3 immunoblot analysis, and MDC staining. *TMEM166* (transmembrane protein 166, also known as FLJ13391) was first identified as a novel gene associated with cell viability in our lab.¹⁰ In our autophagy screen and apoptosis assays, *TMEM166* was identified as a novel regulator involved in both autophagy and apoptosis.²⁹

TMEM74 (transmembrane protein 74) was first identified as a regulator of cell death in a previous study from our lab, and its role in autophagy has been further studied by Dr. Yu in our lab.³⁰

TM9SF1 (transmembrane 9 superfamily member 1, NM_006405.5), also called MP70, is a nine-spanning transmembrane protein first cloned in 1997.²⁹ *TM9SF1* expression is ubiquitous in human tissues, and it is widely expressed and highly conserved among yeast, plants and mammals.³¹ It was reported that *TM9SF1* could be induced by the neurotoxin 6-OHDA in a model of Parkinson's disease in PC12 cells.³² In a recent study of identification tumor-associated antigens,³¹ *TM9SF1* was overexpressed in tumors at levels 5.20 times higher than in normal breast tissue. The same study demonstrated that myc-tagged *TM9SF1* localized to the cell surface of transfected COS-7L cells.³³ However, the function of *TM9SF1* remained unknown until now. Here, we found that *TM9SF1* may play an important role in autophagosome induction. We further found that *TM9SF1*-GFP localized to lysosomes, but not to other membrane compartments in transfected HeLa cells: *TM9SF1*-GFP colocalized extensively with LTR (lysosomal marker) and with DsRed-LC3 (autophagic vacuole marker). Furthermore, knockdown of *TM9SF1* by RNA interference could attenuate autophagosome formation. Collectively, we hypothesized that *TM9SF1* might play a modulating role in the process of autophagy, and then accelerate functional autophagy. But the molecular mechanism is still unclear.

In summary, we have established an effective and convenient cell-based screening platform, which can be applied for high-throughput genomic screening candidate autophagy-related genes using human cDNA and/or siRNA libraries. Three genes (*TMEM74*, *TMEM166* and *TM9SF1*) were identified as positive genes which overexpression can induce autophagosome formation. *TM9SF1* was further investigated as a novel autophagy-related gene. Further studies will be required to elucidate the specific role of *TM9SF1* in autophagy.

Materials and Methods

Materials. We generated rabbit anti-LC3 polyclonal antibodies using recombinant rat LC3 protein expressed in *E. coli* as the antigen, followed by affinity purification and validation by ELISA and immunoblot analysis. Monoclonal antibodies against β -actin and GFP were purchased from Santa Cruz Biotechnology Inc., (USA). HRP-conjugated secondary antibodies against mouse and rabbit IgG were purchased from Cell Signaling (USA). LysoTracker Red (LTR) and MitoTracker Red (MTR) were purchased from Molecular Probes (USA). Earle's Balanced Salt Solution (EBSS) and Bafilomycin A1 and wortmannin were purchased from Sigma (USA). Polyclonal antibody against *TM9SF1* and Cathepsin D were purchased from Aviva Systems Biology (USA) and Santa Cruz (USA), respectively.

The vector for expression of GFP-LC3 was kindly provided by Dr. Zhenyu Yue (Mount Sinai School of Medicine, New York). The vector for expression of mutant GFP-LC3(G120A) was kindly

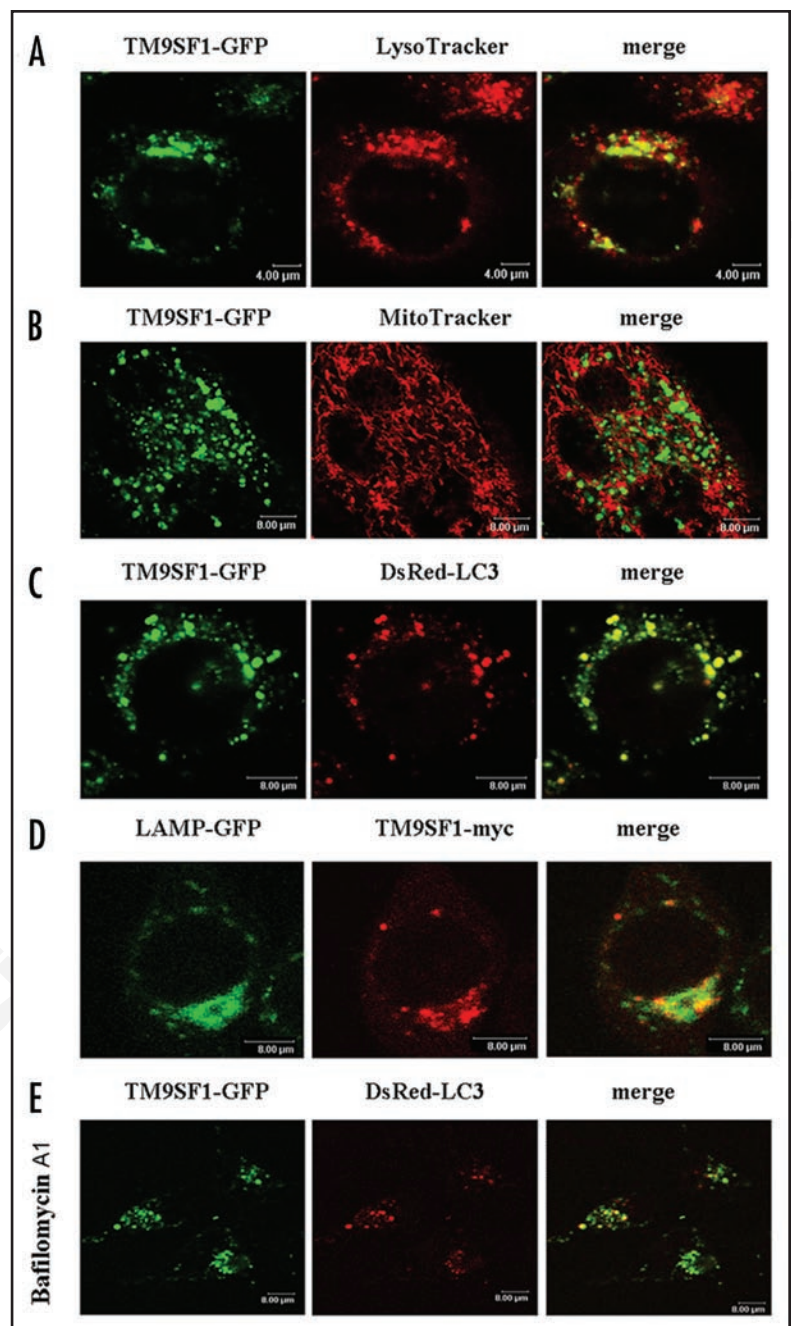


Figure 4. Subcellular localization of *TM9SF1*. For (A) LTR or (B) MTR labeling, HeLa cells were transfected with *TM9SF1*-GFP. At 24 h post-transfection, HeLa cells were probed with LTR or MTR and were analyzed using two-color confocal microscopy. (C) For DsRed-LC3 studies, HeLa cells were cotransfected with *TM9SF1*-GFP and DsRed-LC3. At 24 h posttransfection, HeLa cells were analyzed using two-color confocal microscopy. As shown in the merged image, *TM9SF1* colocalized extensively with LTR and DsRed-LC3, but not with MTR. (D) Cells were transiently transfected with *TM9SF1*-myc and LAMP1-GFP. 24 h after transfection, cells were stained by indirect immunofluorescence with anti-myc antibody and analyzed by confocal microscopy. (E) *TM9SF1*-GFP and DsRed-LC3 were cotransfected into cells. Cells were incubated with 100 nM Bafilomycin A1 for 2 h and analyzed by confocal microscopy.

provided by Dr. Tamotsu Yoshimori (Osaka University, Japan). The vector for expression of DsRed-LC3 was constructed by inserting the PCR-amplified LC3 coding sequence from GFP-LC3 into the in-frame restriction site of the DsRed vector. *TM9SF1*-GFP were constructed by inserting the coding sequence of *TM9SF1* into the

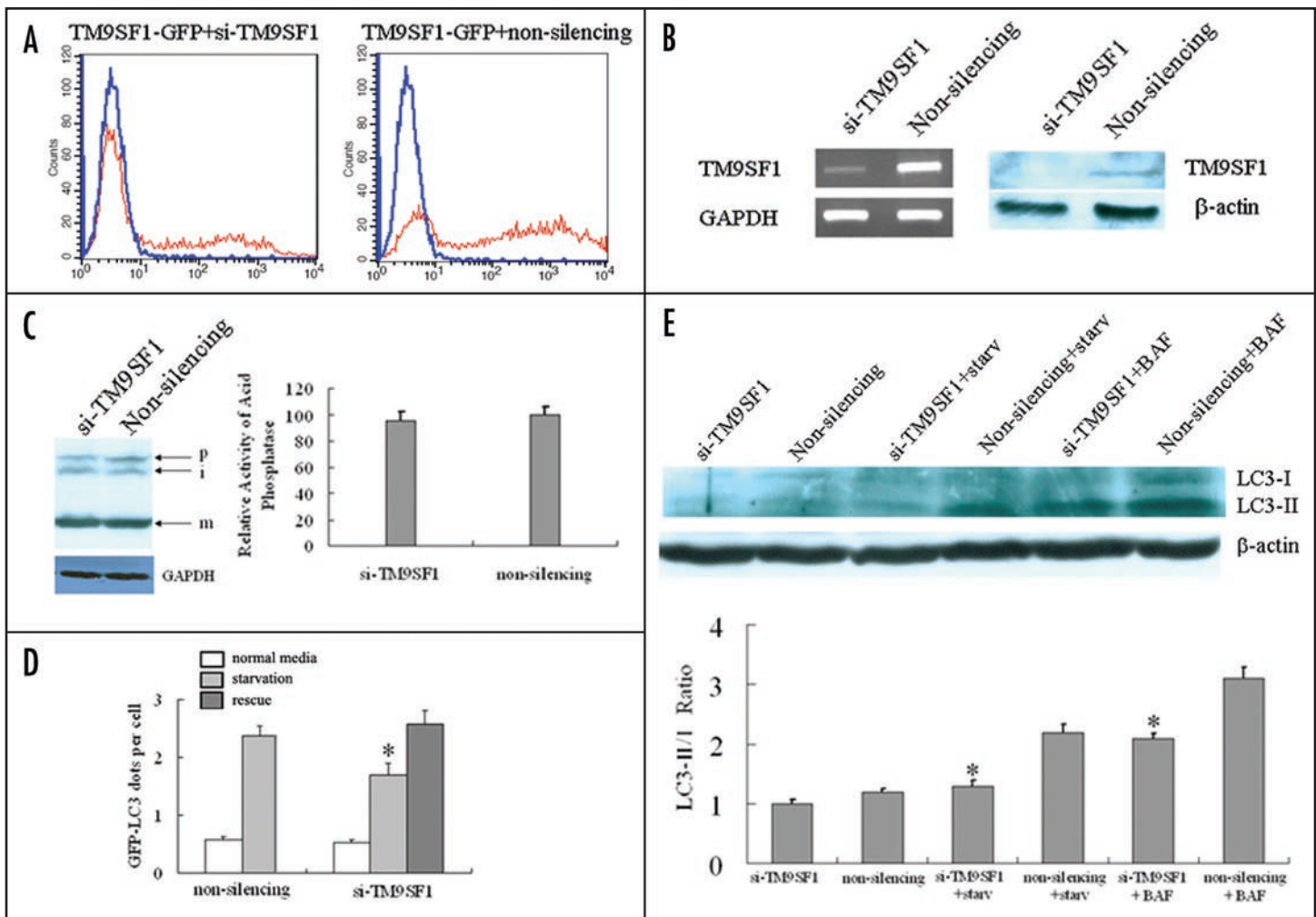


Figure 5. Knockdown of *TM9SF1* inhibits starvation-induced autophagy. (A) si-TM9SF1 inhibited the expression of TM9SF1-GFP fusion protein in HeLa cells. HeLa cells were cotransfected with si-TM9SF1 (or nonsilencing siRNA) and TM9SF1-GFP by electroporation. Fluorescent intensity was analyzed by flow cytometry 48 h after transfection. Fluorescent intensity of cells transfected with si-TM9SF1 decreased over 80% compared with nonsilencing siRNA. Blue curve represent control cells (normal HeLa cells without GFP transfection). (B) Si-TM9SF1 inhibited TM9SF1 mRNA or protein expression. HeLa cells were transfected with si-TM9SF1 (or nonsilencing siRNA). 48 h later, mRNA or protein was prepared for RT-PCR or immunoblotting analysis respectively. (C) Western blotting of cathepsin-D from nonsilencing and si-TM9SF1 transfected HeLa cells. p, precursor; i, intermediate and m, mature form of the enzyme. Equal amounts of protein were loaded in each lane. Total proteins of nonsilencing and si-TM9SF1 transfected HeLa cells were extracted and their lysates were used to measure the lysosomal acid phosphatase enzymatic activity. Data represents the mean \pm SD of three independent experiments. (D) Si-TM9SF1 attenuated the increment of GFP-LC3 punctate cells in starved HeLa cells. HeLa cells were transfected with GFP-LC3 and nonsilencing or si-TM9SF1 and cultured under the standard starvation protocol. After starvation, si-TM9SF1 transfected cells were rescued by transient transfection with knockdown-resistant TM9SF1-myc. The average number of GFP-LC3 dots per cell was determined and expressed as the mean \pm SD of three independent experiments. * Significantly different than control, $p < 0.05$. (E) Si-TM9SF1 decreased the ratio of LC3-II/LC3-I in starved HeLa cells. HeLa cells were transfected with non-silencing siRNA or si-TM9SF1. 48 h after transfection, cells were starved for 2 h or treated with Bafilomycin A1 and then were lysed for immunoblot analysis. The ratio of cellular LC3-II/LC3-I are shown as the mean \pm SD of three independent experiments. * Significantly different than control, $p < 0.05$.

in-frame restriction site of pcDNA.3.1/myc-His(-)B (Invitrogen, USA) and EGFP-N1 (Clontech, USA), respectively. To construct a plasmid expressing knockdown-resistant TM9SF1-myc, base substitutions were made by site-specific mutagenesis employing the overlap extension method and confirmed by DNA sequencing.

cDNA library construction. A human cDNA library was constructed as described previously.¹⁰ A total of 1,050 human ORFs was generated for use in various cell-based functional screening approaches.^{10,11} Our library consisted primarily of cDNAs encoding proteins of unknown function or with poorly defined functions; the role of most of these genes is still not known (Suppl. Table 1).

Cell culture and transfection. HeLa (ATCC CCL-2) cells were cultured in Dulbecco's modified Eagle's medium (DMEM) (Invitrogen, USA) supplemented with 10% fetal calf serum (FCS) (Invitrogen, USA) at 37°C in a 5% CO₂ atmosphere. HeLa cells were cultured in 96-well plates at a density of 10,000 cells/well for the cell-based screening assays to examine GFP-LC3 localization. Twenty-four hours after plating, 90 ng of candidate plasmid DNA was cotransfected with 60 ng of GFP-LC3 plasmid DNA in each well using VigoFect (Vigorous, China), a nonliposomal cationic reagent, according to the manufacturer's instruction. For immunoblot analyses, confocal microscopy assays or electron microscopy

assays, cells were electroporated for 20 ms at 120 V using 10 µg of plasmid DNA per 2×10^6 cells in 2 mm gap cuvettes using an ECM 830 Square Wave Electroporation System (BTX, USA). At 24 h post-transfection, HeLa cells were used in a biochemical and cell biological assays.

Quantitative analysis of GFP-LC3 dots. GFP-LC3-transfected cells cultured in 96-well plates were viewed using a 20x objective lens and autoscanned using an automated fluorescent microscope (Axiovert 200M, Zeiss, Germany) equipped with computer software-driven commands including “scan multiwell plate” and “auto focus” (MetaMorph 7.0 Imaging System, Molecular Devices, USA) (Fig. 1A). Exposure times were set at 300 ms, the number of punctate dots of GFP-LC3 signal per cell in GFP-LC3-positive cells was determined using the “granularity” application module of the MetaMorph 7.0 Imaging System (Fig. 1B). The “granularity” application module is designed to detect and count granules in cells and to measure the physical characteristics of granules (such as area and intensity), which can determine the average number of granules per cell directly. The number of GFP-LC3 dots per cell was counted in at least two independent visual fields from two independent wells. The results were expressed as the average number of GFP-LC3 dots in each cell (mean \pm SD).

Confocal microscopy. HeLa cells transfected with *TM9SF1* or *TM9SF1*-GFP were grown on coverslips, and stained with 200 nM LTR for 15 min, 100 nM MTR for 15 min, or 0.05 mM Monodansylcadaverine (MDC) for 1 h at 37°C; cells were washed three times with PBS and observed using a Leica TCS SP2 Confocal System (Heidelberg, Germany) equipped with the appropriate filters. HeLa cells cotransfected with *TM9SF1*-GFP and DsRed-LC3 were observed directly using the same confocal system. For myc-tagged *TM9SF1*, indirect immunofluorescence assay was used.

Electron microscopy analysis. HeLa cells cultured on coverslips were prefixed in 4% glutaraldehyde in PBS at 4°C, treated with 1% OsO_4 for 2 h at 4°C, dehydrated in a graded series of ethanol, and flat embedded in epon. Ultrathin sections were stained with uranyl acetate and lead citrate, and examined with a JEM-1230 transmission electron microscope (JEOL, Japan). The number of autophagosomes per cell profile was determined by an observer blinded to experimental conditions for a minimum of 50 cells for each specimen.

Immunoblot analysis. Immunoblotting was performed as described previously.¹² Total cell lysates were prepared from HeLa cells, and immunoblotting was performed using different antibodies.

Enzymatic assay. Lysosomal acid phosphatase activity was assayed using 4-methylumbelliferyl phosphate (4-MUP) substrates as described.^{13,14} HeLa cells were lysed with enzyme lysis buffer (50 mM Tris-HCl pH 7.4, 1% Triton-X100, 300 mM NaCl) supplemented with a complete protease inhibitor cocktail (Pierce). The supernatants were incubated at 37°C for 30 min with 1 mM 4-MUP substrate in 0.1 M sodium acetate buffer (pH 4.5), the reaction was stopped by the addition of 0.15 M glycine buffer (pH 10.3), and the fluorescence was measured at Excitation 355 nm/Emission 460 nm by using a GENios Pro reader (Tecan, Switzerland).

***TM9SF1* siRNAs synthesis and electroporation transfection.** Specific siRNA against *TM9SF1* with targeting sequence 5'-GAA TGG CTG AGT CTT TGT A-3' (si-*TM9SF1*) was synthesized by RiboBio Corporation (Guangzhou, China). Nonsilencing siRNA

that had no sequence homology to any known human genes was used as the control. Both siRNAs were dissolved at a concentration of 20 µM in buffer containing 20 mM KCl, 6 mM HEPES, pH 7.5, 0.2 mM MgCl_2 . Cells were fed with fresh culture medium prior to experiments. HeLa cells were electroporated for 20 ms at 120 V, with 10 µg plasmid or 5 µl siRNA per 10^6 cells in 2 mm gap cuvettes using an ECM 830 Square Wave Electroporation System (BTX, USA).

Acknowledgements

We thank Wei Wang from XianFeng Tech., Co., Ltd for his technical assistance in the automated image analysis. We are grateful to Dr. Zhenyu Yue and Dr. Tamotsu Yoshimori for kindly providing GFP-LC3 and mutant GFP-LC3(G120A) plasmids respectively, Dr. Zhendong Zhao for providing recombinant LC3 protein and Dr. Lan Yuan for her assistance in confocal laser scanning microscope. Special thanks to Prof. Chen Yingyu at Peking University Center for Human Disease Genomics for the proofreading the manuscript. This work was supported by a grant from the National High Technology Research and Development Program of China (No. 2006AA02A305).

Note

Supplementary materials can be found at: www.landesbioscience.com/supplement/HeAUTO5-1-Sup.xls

References

- Debnath J, Baehrecke EH, Kroemer G. Does autophagy contribute to cell death? *Autophagy* 2005; 1:66-74.
- Gozuacik D, Kimchi A. Autophagy as a cell death and tumor suppressor mechanism. *Oncogene* 2004; 23:2891-906.
- Levine B. Eating oneself and uninvited guests: autophagy-related pathways in cellular defense. *Cell* 2005; 120:159-62.
- Meijer AJ, Codogno P. Regulation and role of autophagy in mammalian cells. *Int J Biochem Cell Biol* 2004; 36:2445-62.
- Klionsky DJ. The molecular machinery of autophagy: unanswered questions. *J Cell Sci* 2005; 118:7-18.
- Reggiori F, Klionsky DJ. Autophagy in the eukaryotic cell. *Eukaryot Cell* 2002; 1:11-21.
- Mizushima N. Methods for monitoring autophagy. *Int J Biochem Cell Biol* 2004; 36:2491-502.
- Asanuma K, Tanida I, Shirato I, Ueno T, Takahara H, Nishitani T, Kominami E, Tomino Y. MAP-LC3, a promising autophagosomal marker, is processed during the differentiation and recovery of podocytes from PAN nephrosis. *Faseb J* 2003; 17:1165-7.
- Kabeysa Y, Mizushima N, Ueno T, Yamamoto A, Kirisako T, Noda T, Kominami E, Ohsumi Y, Yoshimori T. LC3, a mammalian homologue of yeast Apg8p, is localized in autophagosome membranes after processing. *Embo J* 2000; 19:5720-8.
- Wang L, Gao X, Gao P, Deng W, Yu P, Ma J, Guo J, Wang X, Cheng H, Zhang C, Yu C, Ma X, Lv B, Lu Y, Shi T, Ma D. Cell-Based Screening and Validation of Human Novel Genes Associated with Cell Viability. *J Biomol Screen* 2006; 11:369-76.
- Ma X, Wang X, Gao X, Wang L, Lu Y, Gao P, Deng W, Yu P, Ma J, Guo J, Cheng H, Zhang C, Shi T, Ma D. Identification of five human novel genes associated with cell proliferation by cell-based screening from an expressed cDNA ORF library. *Life Sciences* 2007; 81:1141-51.
- Lv B, Shi T, Wang X, Song Q, Zhang Y, Shen Y, Ma D, Lou Y. Overexpression of the novel human gene, nuclear apoptosis-inducing factor 1, induces apoptosis. *Int J Biochem Cell Biol* 2006; 38:671-83.
- Zhu M, Lovell KL, Patterson JS, Saunders TL, Hughes ED, Friderici KH. Beta-mannosidosis mice: a model for the human lysosomal storage disease. *Hum Mol Genet* 2006; 15:493-500.
- Liang C, Feng P, Ku B, Dotan I, Canaan D, Oh BH, Jung JU. Autophagic and tumour suppressor activity of a novel Beclin1-binding protein UVRAG. *Nat Cell Biol* 2006; 8:688-99.
- Biederick A, Kern HF, Elsasser HP. Monodansylcadaverine (MDC) is a specific *in vivo* marker for autophagic vacuoles. *Eur J Cell Biol* 1995; 66:3-14.
- Bampton ET, Goemans CG, Niranjana D, Mizushima N, Tolkskovy AM. The dynamics of autophagy visualized in live cells: from autophagosome formation to fusion with endo/lysosomes. *Autophagy* 2005; 1:23-36.
- Niemann A, Baltes J, Elsasser H-P. Fluorescence Properties and Staining Behavior of Monodansylpentane, a Structural Homologue of the Lysosomotropic Agent Monodansylcadaverine. *J Histochem Cytochem* 2001; 49:177-86.
- Bagshaw RD, Mahuran DJ, Callahan JW. A proteomic analysis of lysosomal integral membrane proteins reveals the diverse composition of the organelle. *Mol Cell Proteomics* 2005; 4:133-43.

19. Harada JN, Bower KE, Orth AP, Callaway S, Nelson CG, Laris C, Hogenesch JB, Vogt PK, Chanda SK. Identification of novel mammalian growth regulatory factors by genome-scale quantitative image analysis. *Genome Res* 2005; 15:1136-44.
20. Huang Q, Raya A, DeJesus P, Chao S-H, Quon KC, Caldwell JS, Chanda SK, Izpisua-Belmonte JC, Schultz PG. Identification of p53 regulators by genome-wide functional analysis. *P Natl Acad Sci USA* 2004; 101:3456-61.
21. Westbrook TF, Martin ES, Schlabach MR, Leng Y, Liang AC, Feng B, Zhao JJ, Roberts TM, Mandel G, Hannon GJ, Depinho RA, Chin L, Elledge SJ. A genetic screen for candidate tumor suppressors identifies REST. *Cell* 2005; 121:837-48.
22. Kawai A, Takano S, Nakamura N, Ohkuma S. Quantitative monitoring of autophagic degradation. *Biochem Biophys Res Commun* 2006; 351:71-7.
23. Rodríguez-Enriquez S, Kim I, Currin RT, Lemasters JJ. Tracker dyes to probe mitochondrial autophagy (mitophagy) in rat hepatocytes. *Autophagy* 2006; 2:39-46.
24. Klionsky DJ, Cuervo AM, Seglen PO. Methods for monitoring autophagy from yeast to human. *Autophagy* 2007; 3:181-206.
25. Klionsky DJ, Abeliovich H, Agostinis P, Agrawal DK, Aliev G, Askew DS, Baba M, Bachrecke EH, Bahr BA, Ballabio A, Bamber BA, Bassham DC, Bergamini E, Bi X, Biard-Piechaczyk M, Blum JS, Bredesen DE, Brodsky JL, Brumell JH, Brunk UT, Bursch W, Camougrand N, Cebollero E, Cecconi F, Chen Y, Chin LS, Choi A, Chu CT, Chung J, Clarke PG, Clark RS, Clarke SG, Clavé C, Cleveland JL, Codogno P, Colombo MI, Coto-Montes A, Cregg JM, Cuervo AM, Debnath J, Demarchi F, Dennis PB, Dennis PA, Deretic V, Devenish RJ, Di Sano F, Dice JF, Difiglia M, Dinesh-Kumar S, Distelhorst CW, Djavaheri-Mergny M, Dorsey FC, Dröge W, Dron M, Dunn WA Jr, Duszzenko M, Eissa NT, Elazar Z, Esclatine A, Eskelinen EL, Fésüs L, Finley KD, Fuentes JM, Fueyo J, Fujisaki K, Galliot B, Gao FB, Gewirtz DA, Gibson SB, Gohla A, Goldberg AL, Gonzalez R, González-Estévez C, Gorski S, Gottlieb RA, Häussinger D, He YW, Heidenreich K, Hill JA, Høyer-Hansen M, Hu X, Huang WP, Iwasaki A, Jäättelä M, Jackson WT, Jiang X, Jin S, Johansen T, Jung JU, Kadowaki M, Kang C, Kelekar A, Kessel DH, Kiel JA, Kim HP, Kimchi A, Kinsella TJ, Kiselyov K, Kitamoto K, Knecht E, Komatsu M, Kominami E, Kondo S, Kovács AL, Kroemer G, Kuan CY, Kumar R, Kundu M, Landry J, Laporte M, Le W, Lei HY, Lenardo MJ, Levine B, Lieberman A, Lim KL, Lin FC, Liou W, Liu LF, Lopez-Berestein G, López-Otín C, Lu B, Macleod KF, Malorni W, Martinet W, Matsuoka K, Mautner J, Meijer AJ, Meléndez A, Michels P, Miotto G, Mistiaen WP, Mizushima N, Mograbi B, Monastyrska I, Moore MN, Moreira PI, Moriyasu Y, Motyl T, Münz C, Murphy LO, Naqvi NI, Neufeld TP, Nishino I, Nixon RA, Noda T, Nürnberg B, Ogawa M, Oleinick NL, Olsen LJ, Ozpolat B, Paglin S, Palmer GE, Papassideri I, Parkes M, Perlmutter DH, Perry G, Piacentini M, Pinkas-Kramarski R, Prescott M, Proikas-Cezanne T, Raben N, Rami A, Reggiori F, Rohrer B, Rubinsztein DC, Ryan KM, Sadoshima J, Sakagami H, Sakai Y, Sandri M, Sasakawa C, Sass M, Schneider C, Seglen PO, Seleverstov O, Settleman J, Shacka JJ, Shapiro IM, Sibirny A, Silva-Zacarin EC, Simon HU, Simone C, Simonsen A, Smith MA, Spanel-Borowski K, Srinivas V, Steeves M, Stenmark H, Stromhaug PE, Subauste CS, Sugimoto S, Sulzer D, Suzuki T, Swanson MS, Tabas I, Takeshita F, Talbot NJ, Tallóczy Z, Tanaka K, Tanaka K, Tanida I, Taylor GS, Taylor JB, Terman A, Tettamaniti G, Thompson CB, Thumm M, Tolkovsky AM, Tooze SA, Truant R, Tumanovska LV, Uchiyama Y, Ueno T, Uzcátegui NL, van der Klei I, Vaquero EC, Vellai T, Vogel MW, Wang HG, Webster P, Wiley JW, Xi Z, Xiao G, Yahalom J, Yang JM, Yap G, Yin XM, Yoshimori T, Yu L, Yue Z, Yuzaki M, Zabirnyk O, Zheng X, Zhu X, Deter RL. Guidelines for the use and interpretation of assays for monitoring autophagy in higher eukaryotes. *Autophagy* 2008; 4:151-75.
26. Abraham VC, Taylor DL, Haskins JR. High content screening applied to large-scale cell biology. *Trends Biotechnol* 2004; 22:15-22.
27. Carpenter AE, Sabatini DM. Systematic genome-wide screens of gene function. *Nat Rev Genet* 2004; 5:11-22.
28. Tanida I, Minematsu-Ikeguchi N, Ueno T, Kominami E. Lysosomal turnover, but not a cellular level, of endogenous LC3 is a marker for autophagy. *Autophagy* 2005; 1:84-91.
29. Wang L, Yu C, Lu Y, He P, Guo J, Zhang C, Song Q, Ma D, Shi T, Chen Y. TMEM166, a novel transmembrane protein, regulates cell autophagy and apoptosis. *Apoptosis* 2007; 12:1489-502.
30. Yu C, Wang L, Lv B, Lu Y, Zeng L, Chen Y, Ma D, Shi T, Wang L. TMEM74, a lysosome and autophagosome protein, regulates autophagy. *Biochem Biophys Res Commun* 2008; 369:622-9.
31. Chluba-de Tapia J, de Tapia M, Jaggin V, Eberle AN. Cloning of a human multispinning membrane protein cDNA: evidence for a new protein family. *Gene* 1997; 197:195-204.
32. Schlegel J, Neff F, Piontek G. Serial induction of mutations by ethylnitrosourea in PC12 cells: a new model for a phenotypical characterization of the neurotoxic response to 6-hydroxydopamine. *J Neurosci Methods* 2004; 137:215-20.
33. Di Cristina M, Minenkova O, Pavoni E, Beghetto E, Spadoni A, Felici F, Gargano N. A novel approach for identification of tumor-associated antigens expressed on the surface of tumor cells. *Int J Cancer* 2007; 120:1293-303.